Complementary, Selective PET Imaging of Integrin Subtypes $\alpha_5\beta_1$ and $\alpha_v\beta_3$ Using ^{68}Ga-Aquibeprin and ^{68}Ga-Avebetrin

Johannes Notni[1], Katja Steiger[2], Frauke Hoffmann[1], Dominik Reich[1], Tobias G. Kapp[3], Florian Rechenmacher[3], Stefanie Neubauer[3], Horst Kessler[3], and Hans-Jürgen Wester[1]

[1]Lehrstuhl für Pharmazeutische Radiochemie, Technische Universität München, Garching, Germany; [2]Institute of Pathology, Technische Universität München, Munich, Germany; and [3]Institute for Advanced Study and Center of Integrated Protein Science, Department Chemie, Technische Universität München, Munich, Germany

Despite in vivo mapping of integrin $\alpha_v\beta_3$ expression being thoroughly investigated in recent years, its clinical value is still not well defined. For imaging of angiogenesis, the integrin subtype $\alpha_5\beta_1$ appears to be a promising target, for which purpose we designed the PET radiopharmaceutical ^{68}Ga-aquibeprin. **Methods:** ^{68}Ga-aquibeprin was obtained by click-chemistry (CuAAC) trimerization of a $\alpha_5\beta_1$ integrin–binding pseudopeptide on the triazacyclononane-triphosphinate (TRAP) chelator, followed by automated ^{68}Ga labeling. Integrin $\alpha_5\beta_1$ and $\alpha_v\beta_3$ affinities were determined in enzyme linked immune sorbent assay on immobilized integrins, using fibronectin and vitronectin, respectively, as competitors. M21 (human melanoma)-bearing severe combined immunodeficient mice were used for biodistribution, PET imaging, and determination of in vivo metabolization. The expression of α_5 and β_3 subunits was determined by immunohistochemistry on paraffin sections of M21 tumors. **Results:** ^{68}Ga-aquibeprin shows high selectivity for integrin $\alpha_5\beta_1$ (50% inhibition concentration [IC_{50}] = 0.088 nM) over $\alpha_v\beta_3$ (IC_{50} = 620 nM) and a pronounced hydrophilicity (log D = –4.2). Severe combined immunodeficient mice xenografted with M21 human melanoma were found suitable for in vivo evaluation, as M21 immunohistochemistry showed not only an endothelial and strong cytoplasmatic expression of the β_3 integrin subunit but also an intense expression of the α_5 integrin subunit particularly in the endothelial cells of intratumoral small vessels. Ex vivo biodistribution (90 min after injection) showed high uptake in M21 tumor (2.42 ± 0.21 percentage injected dose per gram), fast renal excretion, and low background; tumor-to-blood and tumor-to-muscle ratios were 10.6 ± 2.5 and 20.9 ± 2.4, respectively. ^{68}Ga-aquibeprin is stable in vivo; no metabolites were detected in mouse urine, blood serum, kidney, and liver homogenates 30 min after injection. PET imaging was performed for ^{68}Ga-aquibeprin and the previously described, structurally related c(RGDfK) trimer ^{68}Ga-avebetrin, which shows an inverse selectivity for integrin $\alpha_v\beta_3$ (IC_{50} = 0.22 nM) over $\alpha_5\beta_1$ (IC_{50} = 39 nM). In vivo target specificity was proven by cross-competition studies; tumor uptake of either tracer was not affected by the coadministration of 40 nmol (~5 mg/kg) of the respective other compound. **Conclusion:** ^{68}Ga-aquibeprin and ^{68}Ga-avebetrin are recommendable for complementary mapping of integrins $\alpha_5\beta_1$ and $\alpha_v\beta_3$ by PET, allowing for future studies on the role of these integrins in angiogenesis, tumor progression, metastasis, and myocardial infarct healing.

For correspondence or reprints contact: Johannes Notni, Lehrstuhl für Pharmazeutische Radiochemie, Technische Universität München, Walther-Meissner-Strasse 3, D-85748 Garching, Germany.
E-mail: johannes.notni@tum.de
Published online Dec. 3, 2015.

Key Words: angiogenesis; positron emission tomography; ^{68}Ga; integrins; immunohistochemistry

J Nucl Med 2016; 57:460–466
DOI: 10.2967/jnumed.115.165720

Integrins are a family of cellular transmembrane receptors, always forming dimers by combining 1 of 18 α-chains with 1 of 8 β-chains. They mediate cell adhesion to other cells or proteins of the extracellular matrix, such as fibronectin or vitronectin (*1*). Among the 28 known subtypes, 10 have been shown to play a role in vasculogenesis, angiogenesis, or lymphangiogenesis, of which 6 comprise the β_1 and 3 the α_v chain (*2*). The latter is featured in the most popular integrin, $\alpha_v\beta_3$, which has been extensively exploited as a target for pharmaceuticals and molecular imaging agents (*3–5*) because it was the first integrin recognized to regulate angiogenesis (*6*). In tumors, commencement of this process triggers rapid growth and metastasis (sometimes referred to as angiogenic switch) (*7*). Accordingly, $\alpha_v\beta_3$ integrin antagonists were found to block tumor growth (*6,8*), not only because of inhibition of angiogenesis, but also because cells with unligated or antagonized $\alpha_v\beta_3$ integrin can undergo caspase 8–dependent apoptosis (integrin-mediated death) (*9,10*). Hence, strong efforts were directed toward inhibitors for $\alpha_v\beta_3$ integrin, primarily aiming at antiangiogenic drugs for treatment of cancer (*11*). Among these, cyclic pentapeptides containing the arginine-glycine-aspartic acid sequence (RGD peptides) (*12*) have been extensively used for addressing $\alpha_v\beta_3$ integrin (*13,14*), presumably because of their uncomplicated synthetic accessibility or commercial availability of ready-to-use building blocks. For mapping $\alpha_v\beta_3$ integrin expression in vivo, RGD peptides were equipped with different radionuclides (*15,16*) or fluorophores and used in PET (*17*), SPECT (*18*), or optical imaging (*19*). However, in contradiction to the popular notion of a causal link between uptake of RGD peptides in tissues, $\alpha_v\beta_3$ expression, and angiogenesis, studies on α_v- as well as β_3-deficient mice have shown that both proteins are not strictly required for angiogenesis (*20,21*), and a lack of $\alpha_v\beta_3$ integrin can be compensated for by upregulation of other pathways, such as vascular endothelial growth factor receptor-2 signaling (*22*). On the other hand, $\alpha_v\beta_3$ integrin expression is not restricted to endothelial cells during angiogenesis, but it is also frequently presented on the surface of tumor cells or macrophages. Altogether, collected evidence suggests that $\alpha_v\beta_3$ integrin is neither strictly necessary for angiogenesis, nor is its expression a reliable biomarker for angiogenic activity (*23*).

In contrast to the observations made for β_3, a complete as well as an endothelial cell–specific deletion of the β_1 chain in mice resulted in full inhibition of angiogenesis (*24*). Furthermore, $\alpha_5\beta_1$ integrin is only poorly expressed on quiescent murine and human endothelial cells (*25*) but is upregulated during tumor angiogenesis (*26*). These findings point at a much closer relationship between angiogenesis and expression of integrin $\alpha_5\beta_1$ as compared with $\alpha_v\beta_3$, thus suggesting $\alpha_5\beta_1$ as a more reliable biomarker for activated endothelial cells and angiogenic activity. In view of these prospects, an ^{18}F-labeled cyclic peptide with high affinity for $\alpha_5\beta_1$ integrin was developed but, despite encouraging in vitro data, proved unsuitable for in vivo PET imaging (*27*). Some acyclic pseudopeptides for selective targeting of integrins $\alpha_v\beta_3$ and $\alpha_5\beta_1$ were reported even earlier (*28,29*). Although the corresponding ^{68}Ga-labeled compounds allowed the visualization of expression of both integrins in tumor-xenografted mice (*30*), they showed a considerable amount of unspecific uptake in organs, essentially rendering them less suitable for clinical application.

On the basis of these results, we sought to develop a practicable tool for noninvasive imaging of $\alpha_5\beta_1$ integrin by PET. Beyond that, we considered it of importance to address the expression of both angiogenic-relevant integrins $\alpha_5\beta_1$ and $\alpha_v\beta_3$ in a similar fashion, because for studies seeking to elucidate their role in angiogenesis, their parallel quantification could be highly desirable. Using the triazacyclononane-triphosphinate (TRAP) technology for ^{68}Ga-labeled multimeric bioligands (*31*), we synthesized an $\alpha_5\beta_1$ integrin–targeted trimeric pseudopeptide, ^{68}Ga-aquibeprin, and performed an in vivo cross-validation with the structurally related, $\alpha_v\beta_3$-targeted cyclo(RDGfK) trimer ^{68}Ga-avebetrin (*32*).

MATERIALS AND METHODS

General

Some of the applied experimental protocols have been fully described earlier, namely, ^{68}Ga labeling for rodent experiments (*32*), measurement of log *D* (*33*), determination of integrin affinities (*34*), culture of M21 human melanoma cells and generation of respective xenografts in mice (*33*), biodistribution experiments and determination of in vivo metabolization (*33*), and micro-PET imaging (*32*). Thus, only brief accounts are given here, highlighting alterations made to previously reported procedures. The azide-functionalized $\alpha_5\beta_1$ integrin–targeting pseudopeptide fr306 (*35*), TRAP(alkyne)$_3$ (*31*), and ^{68}Ga-avebetrin (*32*) were synthesized as reported before.

Synthesis of Aquibeprin

TRAP(alkyne)$_3$ (3.7 mg, 4.9 μmol, 1.0 eq.) was added to a solution of sodium ascorbate (9.7 mg, 49 μmol, 10 eq.) in water (50 μL). A solution of the azide-functionalized pseudopeptide fr306 (10.5 mg, 16.1 μmol, 3.3 eq.) in a mixture of MeOH (200 μL) and water (50 μL) was added. After the addition of a solution of $Cu(OAc)_2$ (1.2 mg, 5.9 μmol, 1.2 eq.) in water (50 μL), the reaction mixture was stirred for 3 h and then added to a solution of 1,4,7-triazacyclononane-*N*,*N*′,*N*″-triacetic acid (NOTA, 20 mg, 66 μmol, 13.5 eq.) in dilute aqueous hydrochloric acid (4 mL, 1 μM, pH 3.0) and allowed to stand for 2 d. The demetallation mixture was directly subjected to high-performance liquid chromatography (HPLC) purification. Evaporation and lyophilization of eluate-containing fractions yielded aquibeprin (4.5 mg, 1.5 μmol, 31%) in the form of a colorless solid (molecular weight [calcd.], 2648.76; HPLC [column: Nucleosil 100, 5 μm, RP-C18, 125 × 4.6 mm; flow, 1 mL min^{-1}; gradient, 15%–65% MeCN in H_2O, both containing 0.1% trifluoroacetic acid, in 20 min]; retention time, 8.2 min; mass spectra [electrospray ionization, positive mode]; m/z, 1,325.5 $[M+2H^+]^{2+}$, 884.2 $[M+3H^+]^{3+}$). The $^{nat}Ga^{III}$ complex was obtained by mixing equal amounts of 0.1 mM aqueous solutions of aquibeprin and $Ga(NO_3)_3$, and its immediate and complete formation was confirmed by electrospray ionization-mass spectra (m/z, 1,358.6 $[M+2H^+]^{2+}$, 906.3 $[M+3H^+]^{3+}$). HPLC traces and mass spectra are reported in Supplemental Figures 1–3 (supplemental materials are available at http://jnm.snmjournals.org).

Radiochemistry

With a fully automated system (GallElut$^+$; Scintomics GmbH) as described (*33*), nonprocessed eluate of a ^{68}Ge/^{68}Ga-generator with SnO_2 matrix (IThemba LABS, SA; 1.25 mL, 1 M HCl; total ^{68}Ga activity, 600–700 MBq) was adjusted to pH 2 by adding *N*-(2-hydroxyethyl)piperazine-*N*′-(2-ethanesulfonic acid) buffer (260 mg) and used for labeling of 0.3 nmol aquibeprin or avebetrin, respectively, for 5 min at 95°C. Purification was done by solid-phase extraction using a SepPak C8 light cartridge. The specific activities of tracers thus produced were always greater than 1,000 GBq/μmol (typically 1,300–1,800 GBq/μmol, 30 min after start of elution). Determination of radiochemical purity was done by radio–thin-layer chromatography, using instrumentation as described before (*32*), on Agilent instant thin-layer chromatography silica gel material (eluents, 0.1 M trisodium citrate [$R_f = 0$] and a 1:1 [v/v] mixture of 1 M aqueous ammonium acetate solution and methanol [$R_f = 0.2$]). Radio–high-performance liquid chromatography (Chromolith 100 × 4.6 mm column, flow 3 mL/min, gradient 3%–95% MeCN in water [Merck] [both containing 0.1% trifluoroacetic acid] within 10 min; retention time, 4.6 min) was used for quality control and metabolite analyses. log *D* (*n*-octanol/phosphate-buffered saline, pH 7.4) was determined by the shake-flask method as described previously (*33*).

Integrin Affinities

Affinities of ^{nat}Ga-aquibeprin and ^{nat}Ga-avebetrin for the integrins $\alpha_5\beta_1$, $\alpha_v\beta_3$, and $\alpha_{IIb}\beta_3$ were determined in a solid-phase binding assay according to a previously described method (*34*). Briefly, after coating the corresponding extracellular matrix protein ($\alpha_5\beta_1$, fibronectin; $\alpha_v\beta_3$, vitronectin; $\alpha_{IIb}\beta_3$, fibrinogen) on a plate, a mixture of the ligand and soluble integrin ($\alpha_5\beta_1$, $\alpha_v\beta_3$, or $\alpha_{IIb}\beta_3$, respectively) was added. The integrin ligand was competing with the immobilized extracellular matrix protein for binding to the integrin. Subsequently, surface-bound integrin was detected by specific antibodies in an enzyme-linked immune sorbent assay. All activities were referenced to the activities of the internal standards cilengitide (*36*) ($\alpha_5\beta_1$, 0.54 nM; $\alpha_v\beta_3$, 15.4 nM) and tirofiban ($\alpha_{IIb}\beta_3$, 1.2 nM).

Cell Lines and Animal Model

M21 human melanoma cells (*37*) were cultivated as previously described (*33*) in RPMI 1640 medium, supplemented with 10% fetal bovine serum and 1% gentamicin (all from Biochrom AG) at 37°C in a humidified atmosphere containing 5% CO_2. Tumor xenografts were generated by injecting approximately 1.5×10^7 cells, suspended in serum-free medium supplemented with Matrigel (#354262; Corning), into the right shoulder of 6- to 8-wk-old, female SCID mice (CB17; Charles River). When tumors had grown to a diameter of 6–8 mm (usually 2–3 wk after inoculation), animals were subjected to PET studies or used for biodistribution. All animal experiments were approved by the local authorities and performed in accordance with current animal welfare regulations in Germany.

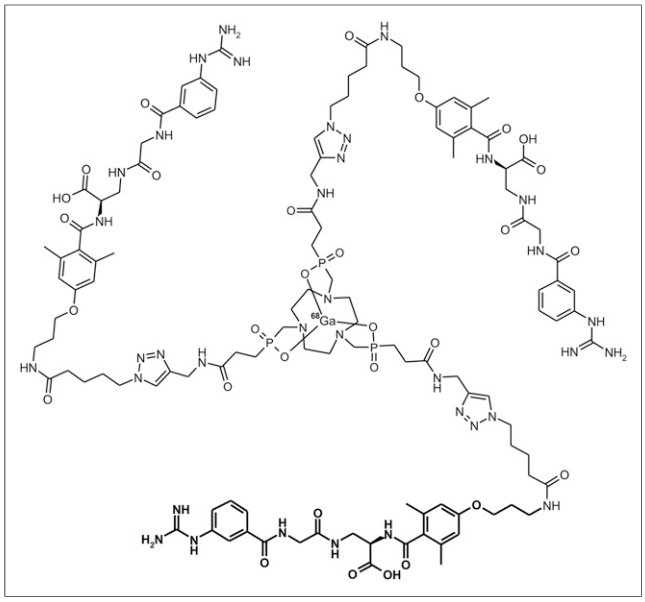

FIGURE 1. Structure of ^{68}Ga-aquibeprin. One of 3 identical $\alpha_5\beta_1$ integrin–binding pseudopeptide substructures is highlighted in boldface.

In Vivo Stability

Determination of metabolites was done according to a previously reported protocol (*32*), for SCID mice administered 40 MBq of ^{68}Ga-aquibeprin. Briefly, animals were sacrificed 30 min after injection, whereafter liver and kidney samples were homogenized and extracted with phosphate-buffered saline. The extracts and a blood sample were centrifuged at 11.500*g*, the supernatants and urine ultrafiltered (molecular weight cutoff, 30 kDa), and filtrates analyzed using reversed-phase HPLC.

Biodistribution and PET Studies

M21-bearing mice were administered 5–7 MBq (4–10 pmol) of ^{68}Ga-aquibeprin for biodistribution, or approximately 20 MBq (13–20 pmol) of ^{68}Ga-aquibeprin or ^{68}Ga-avebetrin for PET, via the tail vein under isoflurane anesthesia. To achieve injections with constant specific activity (or, more precisely, constant amounts of biologically active compound), 1.1 nmol of cold standard were added to each syringe and the actually injected total amount of cold mass calculated from syringe activities before and after injection (typically ~1 nmol due to residuals remaining in the syringes). For blockade, 40 nmol of unlabeled precursor were added to each syringe.

For biodistribution, animals were sacrificed after 90 min, and organs harvested were weighed and the activity contained therein counted in a γ-counter. Calculation of injected dose per gram of tissue was done from organ weights and counted activities, based on individually administered doses. For dynamic PET scans (time–activity curves), animals were injected on-bed, and list-mode data were recorded for 90 min after the injection. For static scans, animals were allowed to wake up with access to food and water, and PET was recorded 75 min after injection for 20 min. Reconstruction and data processing were done as described (*32*).

Immunohistochemistry

For histology and immunohistochemistry, tumors were fixed in 10% neutral-buffered formalin and routinely embedded in paraffin. Sections (2 μm) were cut and stained with hematoxylin and eosin to validate tumor morphology. Consecutive slides were used to detect the expression of integrin subunits immunohistochemically within tumor tissue. After heat-induced antigen retrieval (10 mM citrate buffer, pH 6), unspecific protein and peroxidase binding was blocked with 3% hydrogen peroxide and 3% normal goat serum (Abcam). Immunohistochemistry was performed with an autostainer (DAKO) using antibodies against the α_5 subunit (1:100; b6179 [LSBio]), the β_3 subunit (1:200; 75872 [Abcam]), and CD31 (1:50; 28364 [Abcam]) to visualize intratumoral vascular endothelium. Unspecific staining was excluded using negative control slides incubated without primary antibodies. For antibody detection, the Envision-horseradish peroxidase rabbit–labeled polymer (DAKO) was used, visualized by diaminobenzidine (BS04-500; Immunologic). Counterstaining was performed with hematoxylin.

RESULTS

Aquibeprin Synthesis and Radiochemistry

Aquibeprin was prepared by trimerization of an azide-functionalized pseudopeptide (*35*), using our 1-pot click-chemistry procedure with a tris-alkyne–functionalized TRAP chelator scaffold (Supplemental Scheme 1) (*38*). In analogy to previously reported results for ^{68}Ga-avebetrin (formerly named ^{68}Ga-TRAP(RGD)$_3$; Supplemental Scheme 2) (*39*), fully automated ^{68}Ga labeling of 0.3 nmol of aquibeprin was completed within less than 20 min and delivered ^{68}Ga-aquibeprin (Fig. 1) with 94.4% ± 2.3% decay-corrected yield and greater than 99% radiochemical purity (determined by radio–thin-layer chromatography and radio-HPLC; Supplemental Figs. 4 and 5).

Integrin Affinity and Selectivity

Similar to earlier observations made for multimers of integrin-targeting molecules (*40*), the trimer Ga-aquibeprin possesses

TABLE 1
In Vitro Data for ^{68}Ga-Aquibeprin and ^{68}Ga-Avebetrin

Compound	IC_{50} [nM]			log*D*
	$\alpha_v\beta_3$	$\alpha_5\beta_1$	$\alpha_{IIb}\beta_3$	
^{68}Ga/^{nat}Ga-aquibeprin	620 ± 23	0.083 ± 0.013	>10,000	−4.2 ± 0.1
^{68}Ga/^{nat}Ga-avebetrin	0.22 ± 0.05	39 ± 10	>10,000	−3.9 ± 0.1*

*Data taken from Notni et al. (*31*).

Data are integrin affinities (IC_{50}, [nM]) and *n*-octanol–phosphate-buffered saline distribution coefficients (log*D*, pH 7.4) of Ga-labeled compounds, determined by enzyme-linked immune sorbent assay on immobilized integrins against vitronectin ($\alpha_v\beta_3$), fibronectin ($\alpha_5\beta_1$), and fibrinogen ($\alpha_{IIb}\beta_3$).

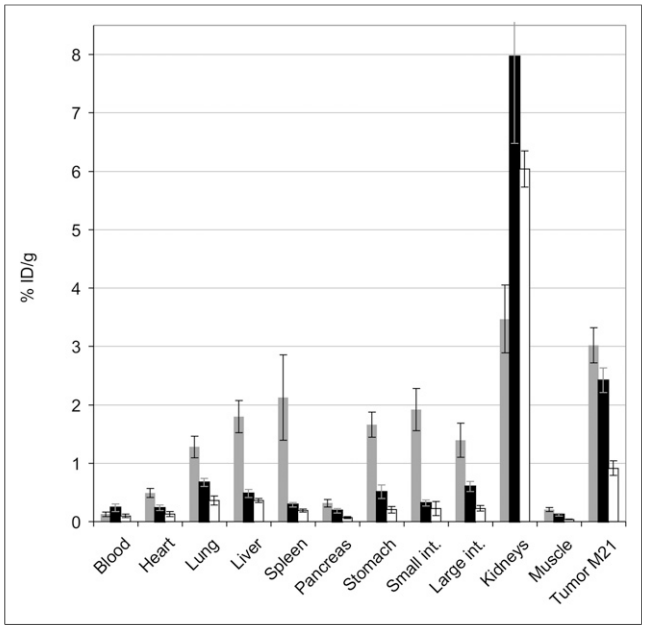

FIGURE 2. Biodistribution in M21 xenografts (90 min after injection, expressed as percentage injected dose per gram of tissue [%ID/g]; mean ± SD) for ^{68}Ga-avebetrin (gray bars, $n = 6$), ^{68}Ga-aquibeprin (black bars, $n = 5$), and ^{68}Ga-aquibeprin with coinjection of 40 nmol (100 μg) aquibeprin (empty bars, $n = 4$) (Supplemental Tables 1 and 2). Int. = intestine.

approximately 16-times-higher affinity than the previously described ^{68}Ga-labeled monomer of the same $\alpha_5\beta_1$-integrin selective pseudopeptide (50% inhibition concentration [IC_{50}] values of 0.083 and 1.3 nM (*30*), respectively; Table 1). The extent of this amplification corresponds well to previous experience with related monomer/TRAP-trimer pairs; for example, an 18-fold enhancement (IC_{50} of 2 and 36 nM) was observed for the trimer and monomer, respectively, of a prostate-specific membrane antigen–targeting peptide (*38*).

Furthermore, the high $\alpha_5\beta_1$ affinity of Ga-aquibeprin does not compromise its specificity. Because of a still-high IC_{50} toward $\alpha_v\beta_3$ (620 nM), its $\alpha_5\beta_1/\alpha_v\beta_3$ affinity quotient of approximately 7,500 is comparable to that of the aforementioned monomer (~7,700) (*30*). With a $\alpha_v\beta_3/\alpha_5\beta_1$ affinity quotient of approximately 180, the inverse selectivity of Ga-avebetrin is less pronounced but sufficient for specific addressing of integrin $\alpha_v\beta_3$. Both compounds show comparable hydrophilicity and do not bind to the platelet integrin $\alpha_{IIb}\beta_3$.

Biodistribution and In Vivo Stability

In M21 tumor, ^{68}Ga-aquibeprin shows slightly lower uptake than ^{68}Ga-avebetrin (2.4 ± 0.2 vs. 3.0 ± 0.3 percentage injected dose per gram, 90 min after injection; Fig. 2). However, the markedly lower organ uptake of ^{68}Ga-aquibeprin (except in the kidneys) results in higher tumor-to-organ ratios than observed for ^{68}Ga-avebetrin. Despite ^{68}Ga-aquibeprin showing somewhat higher uptake in blood, tumor-to-blood and tumor-to-muscle ratios of 10.6 ± 2.5 and 20.9 ± 2.4 percentage injected dose per gram, respectively, illustrate low background activity and high target-to-nontarget contrast (uptake values and tumor-to-organ ratios in numeric form are provided in Supplemental Tables 1 and 2). Competition with 40 nmol (~100 μg or 5 mg/kg) aquibeprin resulted in a marked decrease of all uptake except in the kidneys, indicating that the latter is predominantly related to

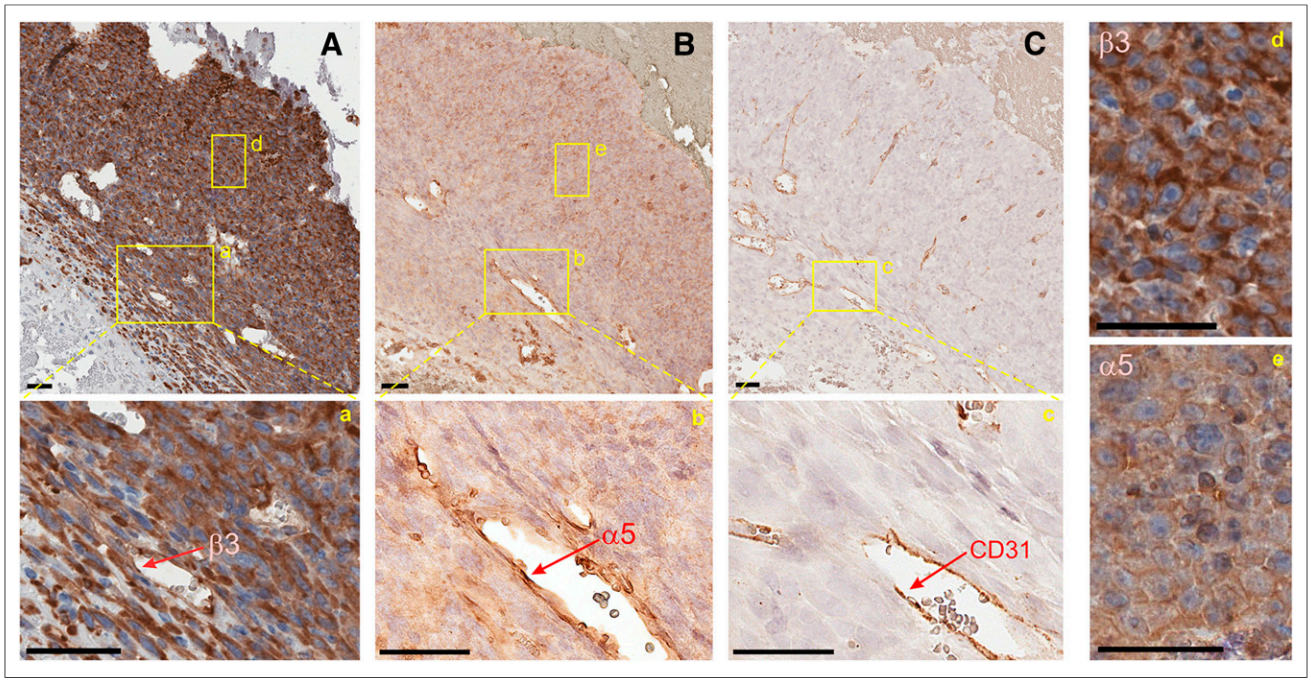

FIGURE 3. Integrin β3 (A, a, d), integrin α5 (B, b), and CD31 (C, c) immunohistochemistry of M21 tumor tissue of same SCID mouse used for PET (Fig. 4). All scale bars shown are 50 μm. α5- and β3-integrin subunits are intensely expressed by endothelial cells of intratumoral small vessels (a, b), as confirmed by CD31 positivity (c). M21 tumor cells show a strong membraneous and cytoplasmic β3 integrin expression (d) and a slight to moderate membraneous α5-integrin expression (e).

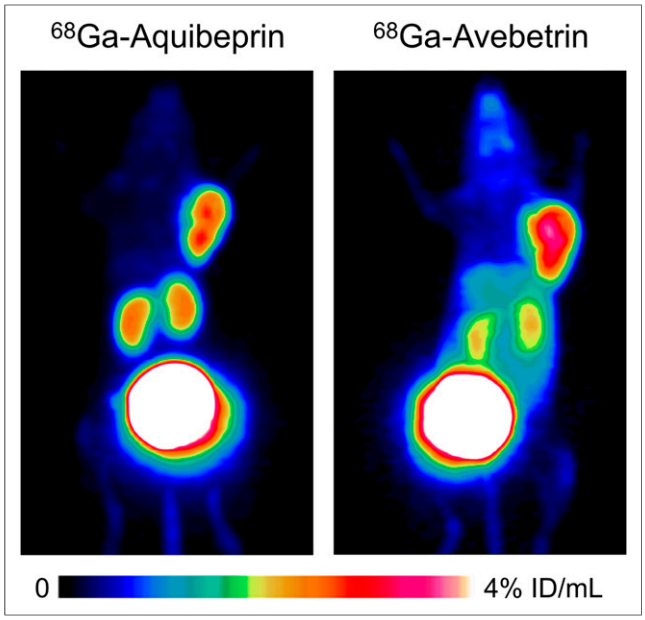

FIGURE 4. PET images (maximum-intensity projection, 75 min after injection) for same M21 human melanoma–xenografted SCID mouse. Time between ^{68}Ga-aquibeprin and ^{68}Ga-avebetrin scans (~20 MBq each) was about 18 h.

excretion. Furthermore, ^{68}Ga-aquibeprin was found to be stable in vivo; no metabolites were found in body fluids and tissue extracts 30 min after injection (Supplemental Fig. 5).

Immunohistochemistry

Immunohistochemistry against the α_5 and the β_3 subunit was used for validation of the expression of the different integrin subunits on the tissue level. The α_5 subunit dimerizes only with β_1, the α_5 immunohistochemistry thus showing exclusively expression of $\alpha_5\beta_1$ integrin. Likewise, β_3 combines only with α_v and α_{IIb}. Because the platelet integrin $\alpha_{IIb}\beta_3$ is not expressed in tissues, it can be assumed that β_3 immunohistochemistry actually reflects $\alpha_v\beta_3$ integrin expression density.

Immunohistochemistry data shown in Figure 3 indicate that both the α_5 and the β3 integrin subunit are intensely expressed by endothelial cells of intratumoral small vessels. Additionally, a slight to moderate membraneous α_5 integrin expression is observed for tumor cells in M21 xenografts. In contrast, integrin β3 shows a much stronger cellular, predominantly cytoplasmic, expression pattern. Overall, a striking similarity of α5 and CD31 staining in consecutive slices demonstrates that expression of integrin α5 is much more confined to endothelial cells than that of integrin β3, rendering integrin α5 a more suitable target for quantification of tumor vascularization by molecular imaging methods than β3.

PET Imaging

Figure 4 shows PET images collected from the same animal whose tumor later underwent immunohistochemistry (Fig. 3), well corresponding with biodistribution data (Fig. 2). ^{68}Ga-aquibeprin uptake in M21 reflects the strong endothelial expression of $\alpha_5\beta_1$ integrin, shown by immunohistochemistry. The somewhat higher overall $\alpha_v\beta_3$ expression is reflected in higher tumor uptake of ^{68}Ga-avebetrin. Furthermore, in accordance with biodistribution data, muscle and organ uptake of ^{68}Ga-aquibeprin is much lower, resulting in markedly improved tumor-to-nontumor contrast.

Figures 5A and 5B show time–activity curves in M21 tumor for ^{68}Ga-aquibeprin and ^{68}Ga-avebetrin, each with and without coinjection of a blocking dose (~5 mg/kg) of the respective other ligand. For both tracers, control and cross-competition curves exhibit no significant differences with respect to the error bands, proving that the respective targets, integrins $\alpha_5\beta_1$ and $\alpha_v\beta_3$, are addressed selectively. In addition, the curve shapes illustrate similar pharmacokinetics, namely high tumor retention and rapid blood clearance (Fig. 5C).

DISCUSSION

In contrast to a previously used experimental setup for evaluating $\alpha_5\beta_1$ integrin–targeting radiopharmaceuticals (*30*), we found in the course of this study that mouse xenografts of the RKO (human colon carcinoma) cell line apparently do not reliably show a constant expression level of integrin $\alpha_5\beta_1$. When using RKO cells for inoculation that underwent greater than 10 passages, uptake of ^{68}Ga-aquibeprin in the resulting tumors was low, pointing at low integrin $\alpha_5\beta_1$ expression. M21 tumors, however, showed high and reproducible ^{68}Ga-aquibeprin uptake. Accordingly, repeated immunohistochemistry analyses of M21 (human melanoma) xenografts consistently showed slight to moderate membraneous integrin $\alpha_5\beta_1$ expression in cells of solid tumors (Fig. 3), rendering this model suitable for evaluation of respective targeted radiopharmaceuticals. Valid results, however, require a quantification of simultaneous $\alpha_v\beta_3$ integrin–mediated uptake, because M21 has been established as an $\alpha_v\beta_3$-expressing cell line (*37*). Hence, this integrin is most practically blocked with a large-dose $\alpha_v\beta_3$-selective ligand during $\alpha_5\beta_1$ imaging to prove selectivity. On inversion, the principle is also applicable for evaluation of tracers addressing $\alpha_v\beta_3$ integrin regarding their selectivity over integrin $\alpha_5\beta_1$. In this way, complementary selectivity of ^{68}Ga-aquibeprin and ^{68}Ga-avebetrin for integrins $\alpha_5\beta_1$ and $\alpha_v\beta_3$, respectively, could be convincingly demonstrated (Figs. 5A and 5B).

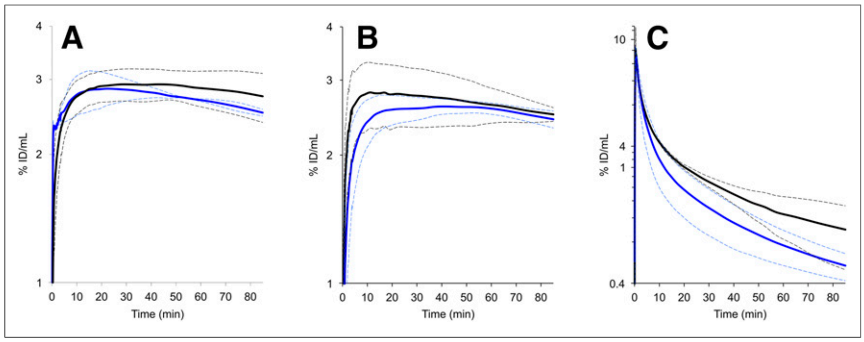

FIGURE 5. Time–activity curves derived from PET data (n = 3, error bands, shown as dotted lines, indicating ±SD). (A) Activity in M21 tumor, ^{68}Ga-aquibeprin without (black) and with coinjection of 40 nmol avebetrin (blue). (B) Activity in M21 tumor, ^{68}Ga-avebetrin without (black) and with coinjection of 40 nmol aquibeprin (blue). (C) Activity in blood, ^{68}Ga-aquibeprin (black) and ^{68}Ga-avebetrin (blue).

It has already been shown that the expression of $\alpha_5\beta1$ integrin and its ligand fibronectin

is upregulated on tumor vasculature. In addition, most blood vessels in tumor sections of human colon and breast carcinoma as well as in subcutaneous xenografts of M21 melanoma cells are $\alpha_5\beta_1$ integrin–positive, whereas endothelial cells in normal tissue do not express this integrin (*26*). Our immunohistochemistry results corroborate and augment these findings, as staining for the endothelial marker CD31 showed a remarkable congruence with α_5 staining (Figs. 3B and 3C), indicating that $\alpha_5\beta1$ integrin indeed is a highly specific target for the detection of neovasculature within tumor tissue.

^{68}Ga-aquibeprin possesses a remarkably high affinity to, and selectivity for, integrin $\alpha_5\beta_1$. Its pronounced hydrophilicity warrants rapid renal clearance from the blood. Biodistribution data indicate a low level of unspecific binding to nontarget organs and tissues, resulting in high-contrast PET imaging. It can be produced quickly (in full automation 15 min plus quality control) and at low cost, independently of an on-site cyclotron. Because of these characteristics, ^{68}Ga-aquibeprin is a practicable tool for in vivo mapping of integrin $\alpha_5\beta_1$ expression and, therefore, angiogenesis by PET, warranting future clinical evaluation.

Moreover, the structurally related tracer ^{68}Ga-avebetrin possesses similar pharmacokinetic properties but selectively addresses integrin $\alpha_v\beta_3$. Because of the short half-life of the nuclide ^{68}Ga (68 min), both radiopharmaceuticals allow for same-day PET imaging of integrins $\alpha_5\beta_1$ and $\alpha_v\beta_3$ in subsequent scans, which is a realistic scenario as their production can be performed rapidly and in the same fashion—that is, using the same robotics and synthetic protocols. Repeated scans could provide valuable information on the time course of expression of both integrins, which offers great potential to further elucidate their multiple biologic functions.

CONCLUSION

Because of their complementary selectivity, ^{68}Ga-aquibeprin and ^{68}Ga-avebetrin constitute a perfectly matched pair of $\alpha_5\beta_1$/$\alpha_v\beta_3$ integrin ligands for in vivo quantification of these integrins. Thus, ^{68}Ga-aquibeprin and ^{68}Ga-avebetrin are recommendable for a wide variety of in vivo studies, for example, on the roles and interplay of integrins $\alpha_5\beta_1$ and $\alpha_v\beta_3$ in angiogenesis and tumor progression, as well as their temporal expression patterns during myocardial infarction healing. Necessity for such work is evident not only from a complete lack of in vivo data on integrin $\alpha_5\beta_1$ expression in humans, but also from the still unclear role of integrin $\alpha_v\beta_3$ in angiogenesis, cancer development, and metastasis (*23*).

DISCLOSURE

The costs of publication of this article were defrayed in part by the payment of page charges. Therefore, and solely to indicate this fact, this article is hereby marked "advertisement" in accordance with 18 USC section 1734. Financial support was provided by the Deutsche Forschungsgemeinschaft (grant NO822/4-1 and SFB 824, projects Z1 and Z2). No other potential conflict of interest relevant to this article was reported.

ACKNOWLEDGMENTS

We thank Prof. Markus Schwaiger (Department of Nuclear Medicine, TUM) for providing laboratory space and granting access to imaging devices and Sybille Reder, Markus Mittelhäuser, and Marco Lehmann for assistance with animal PET.

REFERENCES

1. Margadant C, Monsuur HN, Norman JC, Sonnenberg A. Mechanisms of integrin activation and trafficking. *Curr Opin Cell Biol.* 2011;23:607–614.
2. Avraamides CJ, Garmy-Susini B, Varner JA. Integrins in angiogenesis and lymphangiogenesis. *Nat Rev Cancer.* 2008;8:604–617.
3. Petrillo M, Scambia G, Ferrandina G. Novel targets for VEGF-independent antiangiogenic drugs. *Expert Opin Investig Drugs.* 2012;21:451–472.
4. Seystahl K, Weller M. Is there a world beyond bevacizumab in targeting angiogenesis in glioblastoma? *Expert Opin Investig Drugs.* 2012;21:605–617.
5. Dijkgraaf I, Boermann OC. Radionuclide imaging of tumor angiogenesis. *Cancer Biother Radiopharm.* 2009;24:637–647.
6. Brooks PC, Clark R, Cheresh DA. Requirement of vascular integrin alpha v beta 3 for angiogenesis. *Science.* 1994;264:569–571.
7. Lin EY, Pollard JW. Tumor-associated macrophages press the angiogenic switch in breast cancer. *Cancer Res.* 2007;67:5064–5066.
8. Brooks PC, Strömblad S, Klemke R, Visscher D, Sarkar FH, Cheresh DA. Antiintegrin αvβ3 blocks human breast cancer growth and angiogenesis in human skin. *J Clin Invest.* 1995;96:1815–1822.
9. Stupack DG, Puente XS, Boutsaboualoy S, Storgard CM, Cheresh DA. Apoptosis of adherent cells by recruitment of caspase-8 to unligated integrins. *J Cell Biol.* 2001;155:459–470.
10. Brooks PC, Montgomery AMP, Rosenfeld M, et al. Integrin αvβ3 antagonists promote tumor regression by inducing apoptosis of angiogenic blood vessels. *Cell.* 1994;79:1157–1164.
11. Welti J, Loges S, Dimmeler S, Carmeliet P. Recent molecular discoveries in angiogenesis and antiangiogenic therapies in cancer. *J Clin Invest.* 2013;123:3190–3200.
12. Aumailley M, Gurrath M, Muller G, Calvete J, Timpl R, Kessler H. Arg-Gly-Asp constrained within cyclic pentapeptides: strong and selective inhibitors of cell-adhesion to vitronectin and laminin fragment-P1. *FEBS Lett.* 1991;291:50–54.
13. Meyer A, Auernheimer J, Modlinger A, Kessler H. Targeting RGD recognizing integrins: drug development, biomaterial research, tumor imaging and targeting. *Curr Pharm Des.* 2006;12:2723–2747.
14. Schottelius M, Laufer B, Kessler H, Wester HJ. Ligands for mapping $\alpha_v\beta_3$-integrin expression in vivo. *Acc Chem Res.* 2009;42:969–980.
15. Haubner R, Wester HJ, Reuning U, et al. Radiolabeled $\alpha_v\beta_3$ integrin antagonists: a new class of tracers for tumor targeting. *J Nucl Med.* 1999;40:1061–1071.
16. Haubner R, Wester HJ, Weber WA, et al. Noninvasive imaging of $\alpha_v\beta_3$ integrin expression using ^{18}F-labeled RGD-containing glycopeptide and positron emission tomography. *Cancer Res.* 2001;61:1781–1785.
17. Beer AJ, Kessler H, Wester HJ, Schwaiger M. PET imaging of integrin αvβ3 expression. *Theranostics.* 2011;1:48–57.
18. Zhou YP, Chakraborty S, Liu S. Radiolabeled cyclic RGD peptides as radiotracers for imaging tumors and thrombosis by SPECT. *Theranostics.* 2011;1:58–82.
19. Ye YP, Chen XY. Integrin targeting for tumor optical imaging. *Theranostics.* 2011;1:102–126.
20. Bader BL, Rayburn H, Crowley D, Hynes RO. Extensive vasculogenesis, angiogenesis, and organogenesis precede lethality in mice lacking all αv integrins. *Cell.* 1998;95:507–519.
21. Reynolds LE, Wyder L, Lively JC, et al. Enhanced pathological angiogenesis in mice lacking β3 integrin or β3 and β5 integrins. *Nat Med.* 2002;8:27–34.
22. Reynolds AR, Reynolds LE, Nagel TE, et al. Elevated Flk1 (vascular endothelial growth factor receptor 2) signaling mediates enhanced angiogenesis in β3-integrin deficient mice. *Cancer Res.* 2004;64:8643–8650.
23. Atkinson SJ, Ellison TS, Steri V, Gould E, Robinson SD. Redefining the role(s) of endothelial αvβ3-integrin in angiogenesis. *Biochem Soc Trans.* 2014;42:1590–1595.
24. Fässler R, Meyer M. Consequences of lack of β1 integrin gene expression in mice. *Genes Dev.* 1995;9:1896–1908.
25. Tanjore H, Zeisberg EM, Gerami-Naini B, Kalluri R. β1 integrin expression on endothelial cells is required for angiogenesis but not for vasculogenesis. *Dev Dyn.* 2008;237:75–82.
26. Kim S, Bell K, Mousa SA, Varner JA. Regulation of angiogenesis in vivo by ligation of integrin α5β1 with the central cell-binding domain of fibronectin. *Am J Pathol.* 2000;156:1345–1362.
27. Haubner R, Maschauer S, Einsiedel J, et al. H-CRRETAWAC-OH, a lead structure for the development of radiotracer targeting integrin α5β1? *BioMed Res Int.* 2014;2014:243185.

28. Heckmann D, Laufer B, Marinelli L, et al. Breaking the dogma of the metal-coordinating carboxylate group in integrin ligands: introducing hydroxamic acids to the MIDAS to tune potency and selectivity. *Angew Chem Int Ed Engl.* 2009;48:4436–4440.
29. Rechenmacher F, Neubauer S, Polleux J, et al. Functionalizing αvβ3- or α5β1-selective integrin antagonists for surface coating: a method to discriminate integrin subtypes in vitro. *Angew Chem Int Ed Engl.* 2013;52:1572–1575.
30. D'Alessandria C, Pohle K, Rechenmacher F, et al. In vivo biokinetic and metabolic characterization of the ^{68}Ga-labeled α5β1-selective peptidomimetic FR366. *Eur J Nucl Med Mol Imaging*. October 24, 2015 [Epub ahead of print].
31. Notni J, Šimeček J, Hermann P, Wester HJ. TRAP, a powerful and versatile framework for gallium-68 radiopharmaceuticals. *Chemistry.* 2011;17:14718–14722.
32. Notni J, Pohle K, Wester HJ. Be spoilt for choice with radiolabelled RGD peptides: Preclinical evaluation of ^{68}Ga-TRAP(RGD)$_3$. *Nucl Med Biol.* 2013;40:33–41.
33. Pohle K, Notni J, Bussemer J, Kessler H, Schwaiger M, Beer AJ. ^{68}Ga-NODAGA-RGD is a suitable substitute for ^{18}F-galacto-RGD and can be produced with high specific activity in a cGMP/GRP compliant automated process. *Nucl Med Biol.* 2012;39:777–784.
34. Frank AO, Otto E, Mas-Moruno C, et al. Conformational control of integrin-subtype selectivity in isoDGR peptide motifs: a biological switch. *Angew Chem Int Ed Engl.* 2010;49:9278–9281.
35. Rechenmacher F, Neubauer S, Mas-Moruno C, et al. A molecular toolkit for the functionalization of titanium-based biomaterials that selectively control integrin-mediated cell adhesion. *Chemistry.* 2013;19:9218–9223.
36. Mas-Moruno C, Rechenmacher F, Kessler H. Cilengitide: the first anti-angiogenic small molecule drug candidate—design, synthesis and clinical evaluation. *Anticancer Agents Med Chem.* 2010;10:753–768.
37. Cheresh DA, Spiro RC. Biosynthetic and functional properties of an Arg-Gly-Asp directed receptor involved in human melanoma cell attachment to vitronectin, fibrinogen, and von Willebrand factor. *J Biol Chem.* 1987;262:17703–17711.
38. Baranyai Z, Reich D, Vágner A, et al. Shortcut to high-affinity Ga-68 and Cu-64 radiopharmaceuticals: one-pot click chemistry trimerisation on the TRAP platform. *Dalton Trans.* 2015;44:11137–11146.
39. Notni J, Pohle K, Wester HJ. Comparative gallium-68 labeling of TRAP-, NOTA-, and DOTA-peptides: practical consequences for the future of gallium-68-PET. *EJNMMI Res.* 2012;2:28.
40. Poethko T, Schottelius M, Thumshirn G, et al. Chemoselective pre-conjugate radiohalogenation of unprotected mono- and multimeric peptides via oxime formation. *Radiochim Acta.* 2004;92:317–327.

JNM The Journal of NUCLEAR MEDICINE

Complementary, Selective PET Imaging of Integrin Subtypes $\alpha_5\beta_1$ and $\alpha_v\beta_3$ Using ^{68}Ga-Aquibeprin and ^{68}Ga-Avebetrin

Johannes Notni, Katja Steiger, Frauke Hoffmann, Dominik Reich, Tobias G. Kapp, Florian Rechenmacher, Stefanie Neubauer, Horst Kessler and Hans-Jürgen Wester

J Nucl Med. 2016;57:460-466.
Published online: December 3, 2015.
Doi: 10.2967/jnumed.115.165720

The Journal of Nuclear Medicine is published monthly.
SNMMI | Society of Nuclear Medicine and Molecular Imaging
1850 Samuel Morse Drive, Reston, VA 20190.
(Print ISSN: 0161-5505, Online ISSN: 2159-662X)

SNMMI SOCIETY OF NUCLEAR MEDICINE AND MOLECULAR IMAGING